TISSUE ENGINEERING: Part A
Volume 19, Numbers 19 and 20, 2013

DOI: 10.1089/ten.tea.2012.0650

Marine Collagen Scaffolds for Nasal Cartilage Repair: Prevention of Nasal Septal Perforations in a New Orthotopic Rat Model Using Tissue Engineering Techniques

Christian Bermueller, MD,[1,*] Silke Schwarz, MSc,[1,*] Alexander F. Elsaesser, MSc,[1] Judith Sewing, MSc,[2,3] Nina Baur, MSc,[1] Achim von Bomhard, MD,[1] Marc Scheithauer MD,[1] Holger Notbohm, PhD,[2] and Nicole Rotter, MD[1]

Autologous grafts are frequently needed for nasal septum reconstruction. Because they are only available in limited amounts, there is a need for new cartilage replacement strategies. Tissue engineering based on the use of autologous chondrocytes and resorbable matrices might be a suitable option. So far, an optimal material for nasal septum reconstruction has not been identified. The aim of our study was to provide the first evaluation of marine collagen for use in nasal cartilage repair. First, we studied the suitability of marine collagen as a cartilage replacement matrix in the context of *in vitro* three dimensional cultures by analyzing cell migration, cytotoxicity, and extracellular matrix formation using human and rat nasal septal chondrocytes. Second, we worked toward developing a suitable orthotopic animal model for nasal septum repair, while simultaneously evaluating the biocompatibility of marine collagen. Seeded and unseeded scaffolds were transplanted into nasal septum defects in an orthotopic rat model for 1, 4, and 12 weeks. Explanted scaffolds were histologically and immunohistochemically evaluated. Scaffolds did not induce any cytotoxic reactions *in vitro*. Chondrocytes were able to adhere to marine collagen and produce cartilaginous matrix proteins, such as collagen type II. Treating septal cartilage defects *in vivo* with seeded and unseeded scaffolds led to a significant reduction in the number of nasal septum perforations compared to no replacement. In summary, we demonstrated that marine collagen matrices provide excellent properties for cartilage tissue engineering. Marine collagen scaffolds are able to prevent septal perforations in an autologous, orthotopic rat model. This newly described experimental surgical procedure is a suitable way to evaluate new scaffold materials for their applicability in the context of nasal cartilage repair.

Introduction

Damage or malformation of cartilaginous facial structures, such as the nose or the auricle, may occur as the result of trauma, tumor resection, or congenital defects. Such defects may lead to functional problems, and severe psychosocial strain for the afflicted patient.[1,2]

The limited self-repair capacity[2,3] of cartilage necessitates the use of either autologous transplants, such as rib or auricular cartilage, or synthetic materials, such as Gore-Tex or silicone.[3] The current gold standard for reconstruction of facial cartilage defects is autologous cartilage. In complex defects, multistage surgical procedures are required.[2–4] Donor-site morbidity is common when large pieces of autologous cartilage are harvested.[1,5] Nevertheless, nasal and auricular reconstructions have significant psychosocial benefits in the majority of treated patients.[6]

The use of nonresorbable implants frequently results in infection and/or extrusion of the implant.[7,8] Thus, there continues to be demand for alternative materials.[1,2] Tissue engineering is seen as a promising method for reconstructing auricular and nasal cartilage. Resorbable scaffold materials could be used to accommodate cells. The total mechanical stability of the cell-scaffold construct should not change over time, and the mechanical properties initially exhibited by the biomaterial should be transferred to the newly synthesized matrix *in vivo*. A multitude of different natural and synthetic materials have been tested so far.[9–17] However, none has proven to be optimal[18–20] for the reconstruction of cartilage in the head and neck region. This is mainly due to poor

[1]Department of Otorhinolaryngology, Ulm University Medical Center, Ulm, Germany.
[2]Institute for Virology and Cell Biology, University of Lübeck, Lübeck, Germany.
[3]CRM, Coastal Research & Management, Kiel, Germany.
*These authors equally contributed to this work.

mechanical performance, which is of particular concern in the head and neck area. Additionally, many of the materials can cause local inflammatory reactions.

The particular demands of cartilage reconstruction in head and neck surgery require a specific scaffold design. First, the structural architecture of the scaffold should mimic the exact shape of the native tissue and should support the attachment, proliferation, and differentiation of the desired cell type.[21] Second, the scaffold must be rigid enough to stabilize the reconstructed nasal cartilage until the newly synthesized extracellular matrix (ECM) attains full mechanical stability and function. The cartilaginous septum is responsible for the shape and tension of its surrounding structures (alar cartilages, columella, and nasal dorsum), and these structures in turn enable nasal breathing. Thus, rigidity and stability of the scaffold are of utmost importance.

For many years, collagen has been used as a biomaterial in a variety of connective tissue engineering applications,[22] but collagen has also played an important role in other fields of bioengineering.[23–29] Collagen has many desirable characteristics for scaffold production and application. It provides excellent biocompatibility, low antigenicity, and high biodegradability, and collagen's cell binding and signaling properties help to promote cellular processes leading to tissue formation.[22–24] For this reason, collagen, which may be harvested from bovine skin and bone, is regarded as one of the most favorable materials for artificial ECM replacement.[22] However, because it is harvested from vertebrate animals, it has the disadvantage of potentially carrying transmissible diseases.[22,30]

Most marine animals are invertebrates, so marine collagen is free of substances that would be pathogenic to humans.[30] Several studies have demonstrated that invertebrate fibrillar collagens possess the same characteristics as their human counterparts.[31] Due to their biological properties, new matrices based on marine collagen were recently tested in biomedical applications, such as tissue engineering vascular grafts. Such matrices might represent an alternative source for the production of scaffolds for tissue engineering applications.[30,32–34] Marine collagen is harvested by lyophilization of the invertebrate jellyfish species *Rhopilema esculentum*. Advantages of this collagen source include its reproducible production process, which relies on renewable natural resources, and the absence of any risk for disease transmission by viruses or bacteria.[30]

The other vital part of a tissue-engineered cartilage construct is the cellular component. For clinical applications, access to a suitable source of autologous cells is essential to avoid disease transmission[35] and to avoid a potential immunological rejection caused by an allogenic donor cell source.[36–38] In recent years, hyaline human nasal septum cartilage has been shown to be useful as an alternative autologous cell source because harvesting cartilage from the nasal septum requires minimally invasive surgeries with minimal donor site morbidity.[39] Compared with articular and auricular chondrocytes, nasal septum chondrocytes have been reported to display increased cartilage formation and better mechanical stability in the resulting neo-cartilage.[16,36,38–40]

Aside from biomaterial and donor cell considerations, the nasal septum has specific immunological and mechanical characteristics. The influence of these characteristics can only be analyzed in detail in a suitable animal model.

The goal of this study was to evaluate the biocompatibility of marine collagen *in vitro* and *in vivo* and to determine whether it can be used as a new biomaterial for nasal septum reconstruction. We examined the suitability of marine collagen for growing human and rat nasal septal chondrocytes, and we further aimed to develop a nasal septum-specific immunocompetent animal model to study the effects of site-specific local influences on tissue-engineered cartilage.

Materials and Methods

All experiments were performed with the approval of the Regional Ethical Board in Tuebingen, Germany, administrative decision no. 949/2009.

Marine collagen scaffolds

Triple helical homotrimer marine collagen was harvested from the jellyfish *Rhopilema esculentum*. All steps were carried out at 4°C–6°C. Cured jellyfish was cut into small pieces, rinsed several times with tap water, and washed for several hours in Milli-Q water until the salinity was below 0.01. After equilibration in 0.5 M acetic acid, the material was homogenized in 0.5 M acetic acid. Enzymatic digestion was performed for approximately 70 h using a pepsin solution containing 10 mg g^{-1} basic raw material (porcine gastric mucosa; Biozym). After centrifugation at 17,000 *g* for 30 min, the supernatant was neutralized (pH 7.0) and the collagen was precipitated with 17.5% KCl and 0.2 M NaH_2PO_4. The collagen was obtained by centrifugation for 20 min at 17,000 *g* followed by dialysis against 0.05% acetic acid. Pepsin remained in the supernatant.

For scaffold production, the harvested collagen was freeze-dried (20 mg mL^{-1}), suspended in 0.05% acetic acid, and injected into a preformed synthetic casting mold. Scaffold material was frozen (at a rate of -0.25°C min^{-1}) until it reached -20°C before being freeze-dried. Cross-linking was carried out with 1-ethyl-3-(3-dimethylaminopropyl) carbodiimide (EDC, 0.05/0.15 or 1% w/v EDC in 80% ethanol) for 1.5 h at room temperature. Subsequently, the scaffolds were rinsed several times in Milli-Q water. The reaction was halted by treatment with 1% glycine (w/v in water) overnight, and it was again washed several times before being equilibrated in PBS for use in cell culture.

Scaffold matrices of two different shapes were used for *in vitro* and *in vivo* testing: rectangular marine collagen scaffolds for complete nasal septum replacement, with dimensions of 8×5×2 mm and disc-shaped scaffolds for *in vitro* three dimensional (3D) culture, with a height of 3 mm and a diameter of 6 mm.

Scanning electron microscopy

To visualize the porosity and structure of scaffolds, scanning electron microscopy (SEM) was carried out using a Philips XL 30/ESEM with a field emission gun operated in SEM mode. Dehydrated, freeze-dried samples were fixed on carbon pads and sputter-coated with gold.

Stress-relaxation test

To assess biomechanical properties, stress-relaxation tests were performed according to Stok *et al.*[41] Prior to biomechanical testing, samples were equilibrated for 15 min in PBS

at RT. Measurement of the exact scaffold height and confined compression testing were carried out in a standard materials-testing machine (Zwick, Roell) using a 5 N load cell and an indenter with a diameter of 1.38 mm. The preload was set to 0.1 N. Samples were placed in a cylindrical confining compression chamber containing PBS. Measurements were carried out with a stress-relaxation indentation in three strain steps: 5%, 15%, and 25% of the specimen thickness. After each strain step, the specimens were left to relax for several minutes at that strain until equilibrium was reached. Throughout the testing, force, displacement, and time data were recorded. Subsequent analysis of the E-modulus was performed by using testXpert® software (Zwick, Roell).

Assessment of pore size

For the estimation of pore size, scaffolds were embedded in CryoMolds (Sakura) with the Tissue Tek automated embedding system (Sakura), frozen at −20°C, and cut into 40 μm slices (Leica CM 3050 S; Leica Biosystems). Horizontal sections (each $n=3$) of the middle of the scaffolds ($n=3$) were analyzed by light microscopy. The average pore size is given as the mean ± standard deviation.

Isolation of primary human (hCh) and rat (rCh) nasal septum chondrocytes

Human nasal septum cartilage biopsies were obtained during routine septoplasties and septorhinoplasties in the Department of Otorhinolaryngology, University Medical Center Ulm. Donor age ranged from 18 to 39 years, with an average age of 22 ± 8 (total $n=5$, gender ratio female/male 1/4). Cartilage harvesting was approved by the Ulm University Ethical Committee (No.: 152/08).

Primary rat nasal septum chondrocytes (rCh) were isolated from freshly harvested pieces of rat septum cartilage. Rat and human cartilage samples were rinsed in culture medium: DMEM/Ham's-F12 (Biochrom), supplemented with 10% FBS (Biochrom) and 0.5% gentamicin (PAA). Cartilage was minced and transferred to digestion medium: culture medium containing collagenase type II (0.3%, Worthington). The cartilage was then incubated for 18 h at 37°C in a shaking water bath. Cells were pelleted by centrifugation, and total cell number and vitality were determined. Chondrocytes were seeded at a density of 0.5×10^4 cells cm^{-2}.

When cultures reached 80%–90% confluence, cells were detached by trypsinization, then counted, and cryopreserved to ensure that chondrocytes were treated equally and that only cells in passage 1 were used. To avoid growth factor addition (with a view toward later *in vivo* clinical use), rCh and hCh were amplified in culture medium only. All cell culture experiments were performed at 37°C and 5% CO_2 under humidified conditions.

In vitro *evaluation of marine collagen scaffolds*

Seeding and *in vitro* 3D culture of human and rat chondrocytes. Prior to seeding, marine collagen scaffolds were incubated in culture medium for 24 h to adjust the pH and rehydrate the scaffold matrix. rCh and hCh were thawed and grown to 80%–90% confluence in monolayer culture. Cells were detached and resuspended in culture medium to achieve a final cell concentration of 5.0×10^6 cells mL^{-1}. Five scaffolds were placed together and tightly packed in one well of a 24-well plate, and the scaffolds were seeded by adding 1 mL of cell suspension (equivalent to 1×10^6 cells/scaffold). To enable cell adhesion, seeded scaffolds were incubated for 1 h.

In vitro 3D culturing of hCh and rCh was carried out by using chondrocyte differentiation medium (NH Chondro Diff Medium; Miltenyi) supplemented with 0.5% gentamicin. The medium was supplemented with specific growth factors, but the exact formulation of the medium is proprietary and not disclosed by the provider. Scaffolds seeded with rCh and hCh were analyzed on days 7, 14, and 21.

Cytotoxicity testing. To determine the cytotoxic effects of marine collagen scaffolds, testing was performed using rCh, hCh, and the murine fibrosarcoma cell line L929, as described previously, according to international standard ISO 10993-5:2009.[42]

Quantitative assay for DNA. The number of hCh growing on the marine collagen scaffold surface, and the number growing within the scaffold matrix, was estimated by performing Hoechst assay,[43] as described previously.[44]

Quantitative DMMB-assay for sulfated GAGs. Samples were snap-frozen and freeze-dried (Christ alpha 1–4 freeze dryer). Unseeded and seeded (7, 14, and 21 days, each $n=6$) marine collagen samples were digested overnight in a solution of 50 μg mL^{-1} proteinase K in 100 mM K_2HPO_4 (pH 8.0) at 56°C. Subsequent measurement of sulfated *GAGs* was performed, as recently published[44] and described by Barbosa.[45]

Real-time PCR. The *de novo* synthesis of aggrecan (*ACAN*), collagen type I (*COL1A1*) and II (*COL2A1*), and versican (*VCAN*) by hCh was investigated in long-term 3D culture by analyzing mRNA expression. After 0, 7, 14, and 21 days (each $n=6$), the culture medium was removed, and the RNA of the day 0 monolayer culture chondrocytes was immediately isolated. Seeded scaffolds were snap-frozen and homogenized in 500 μL RLT-buffer (Qiagen) supplemented with β-mercaptoethanol (Sigma) by using a tissue lyser (Qiagen) for 5 min at 50 Hz. RNA was isolated and purified using the RNeasy Mini kit according to the manufacturer's instructions. Harvested RNA was adjusted to a concentration of 50 ng μL^{-1} and kept on ice.

One-step real-time PCR was performed using the Real Time Ready RNA Virus Master Kit (Roche) and Universal Probe Library (UPL, Roche). The primers that were used are shown in Table 1. Reverse transcription was carried out at 58°C for 8 min, and the initial denaturation occurred at 95°C for 30 s. Amplification was performed in two steps for 45 cycles: 95°C for 1 s, followed by 60°C for 20 s. Duplicates of each sample were performed. CP median values were determined using a LightCycler 2.0 (Roche) and the Roche Light Cycler Software version 4.1. Relative gene expression was calculated by using the $2^{-\Delta\Delta CT}$ formula.[46] *GAPDH* was used as a reference gene.

In vivo *evaluation of marine collagen as a cartilage replacement material*

Seeding and 3D culture of rCh on marine collagen matrices prior to *in vivo* biocompatibility evaluation. Three

Table 1. Summary of Investigated Genes, Specific Primers, Expected Fragment Size, and Used Probes

	UPL probe	*Primer left*	*Primer right*	*Amplicon (nt)*
Target gene				
Aggrecan (*ACAN*)	# 79	5′-tgcagctgtcactgtagaaactt-3′	5′-atagcaggggatggtgagg-3′	112
Collagen type I (*COL1A1*)	# 15	5′-atgttcagctttgtggacctc-3′	5′-ctgtacgcaggtgattggtg-3′	126
Collagen type II (*COL2A1*)	# 19	5′-ccctggtcttggtggaaac-3′	5′-tccttgcattactcccaactg-3′	88
Versican (*VCAN*)	# 54	5′-gcacctgtgtgccaggata-3′	5′-cagggattagagtgacattcatca-3′	70
Housekeeping				
GAPDH	# 60	5′-gctctctgctcctcctgttc-3′	5′-acgaccaaatccgttgactc-3′m	115

dimensional culture of marine collagen scaffolds prior to *in vivo* biocompatibility evaluation was carried out by seeding scaffolds with rCh. Seeding and culture was performed as described in the section Assessment of pore size, except that all seeded scaffolds were transferred and cultured in culture medium to avoid the use of growth factors. Scaffolds were precultured for 1 week. Deposition of GAGs after 7 days was compared to unseeded scaffolds and quantified as described in section Quantitative assay for DNA.

Animal model. An inbred strain of Lewis rats was used to minimize the risk of graft rejection due to MHC incompatibility. This approximates the autologous situation. Male Lewis rats (weight: 300–350 g) were anesthetized by the intraperitoneal injection of ketamine (0.5 mg kg^{-1} bodyweight) and xylazine (11.5 mg kg^{-1} bodyweight).

Rats were intubated and fixed in a stereotactic alignment system by using nontraumatic ear bars and an incisor clamp (Small Animal Stereotaxic Instrument, David Kopf Instruments).

After shaving and local skin disinfection, the skin was incised under sterile conditions, and the nasofrontal and nasomaxillary sutures (Fig. 1a) were exposed. After weakening these sutures with a 2 mm diamond burr (PROXXON MICROMOT 50/E Niersbach), a rhinotomy was performed using a 4 mm chisel. The nose was temporarily opened by moving the nasal bones anteriorly, using the fixed skin of the snout as a hinge.

The cartilaginous septum was exposed using 2.3× magnification. The perichondrium was bluntly dissected, and the complete cartilaginous septum was removed (Fig. 1b). Between the two mucoperichondrial flaps, the engineered scaffolds were placed in the original position of the native cartilage. Two drops of xylometazoline solution (0.025% mL^{-1}, OTRIVEN® decongestant nose drops for infants, Novartis) were administered in the wound, the nasal bones were repositioned, and the skin was sutured using DECLENE 5-0.

After 1, 4, and 12 weeks, rats were euthanized, and the whole septal area was assessed by macroscopic, histological, and immunohistochemical analyses.

Experimental groups. We established four experimental groups of animals (Table 2). The first group was implanted with unseeded collagen scaffolds, the second group was implanted with seeded collagen scaffolds. The third group was the so-called "sham-group", in which the nasal septal cartilage was removed and replanted within the same surgery. For the control group, the entire nasal septal cartilage was removed without any replacement (Table 2). The initial number of operated animals per experimental group was 24, to explant eight specimens after each 1, 4, and 12 weeks.

Histological and immunohistochemical analyses

In vitro and *in vivo* samples were fixed in 3.5%–3.7% neutral buffered formalin (Fischar), embedded in paraffin, and sectioned at 3–5 µm. Sections were heat fixated at 56°C for 24 h. Prior to staining, the sections were deparaffinized and rehydrated.

Histological staining. Alcian blue (AB) staining combined with hematoxylin was used to visualize cell migration and cell distribution in the 3D cultured scaffolds, and this staining also enabled detection of newly synthesized acidic sulfated proteoglycans within the explanted matrices and long-term cultured scaffolds.

Immunohistochemical detection of collagen type I, II, and aggrecan. Immunohistochemical staining for collagen type I (anti-rat: ab34710, Abcam, human: Serotec), collagen type II

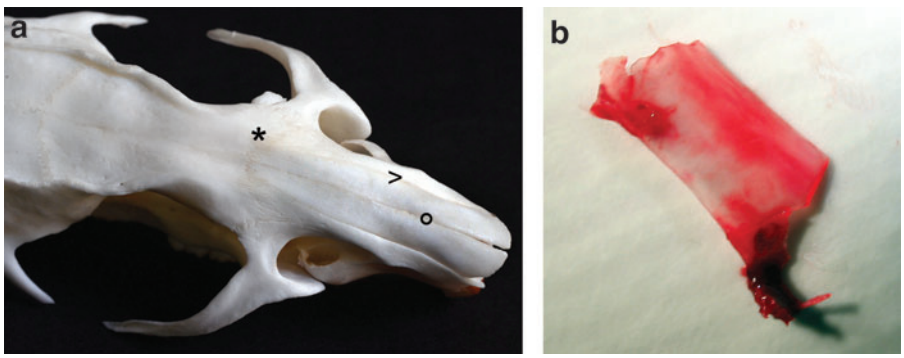

FIG. 1. For orthotopic nasal septum replacement, the nasofrontal (*) and nasomaxillary (>) sutures were exposed and opened, whereas the internasal suture (°) was maintained **(a)**. After detaching the mucosa, the complete nasal septal cartilage was removed **(b)**. Color images available online at www.liebertpub.com/tea

Table 2. Groups and Number of Evaluated Animals ($Animals_{evaluated}$)

Group		Weeks 1[a]	4	12[a]
Unseeded	$animals_{evaluated}$	8	6	8
	+	8	4	3
	−	0	2	5
Seeded	$animals_{evaluated}$	8	7	8
	+	0	3	1
	−	8	4	7
Sham[b]	$animals_{evaluated}$	4	6	8
	+	0	0	0
	−	4	6	8
Control[b]	$animals_{evaluated}$	8	8	7
	+	8	6	5
	−	0	2	2

[a]OR 5% (confidence interval) 0.21 (0.05–0.96); $p < 0.05$.
[b]OR 5% (confidence interval) 0.03 (0.01–0.16); $p < 0.01$.
+, number of animals with perforation, −, number of animals without perforation after the respective implantation time of 1, 4, and 12 weeks.

(anti-rat and anti-human: II-II6B3; Developmental Studies Hybridoma Bank), and aggrecan (anti-rat: Millipore, anti-human: Serotec) was performed by using the LSAB + System-HRP (Dako) and AEC chromogen (Dako).

In brief, for detection of collagen type I, sections were digested with proteinase K for 5 min, and subsequently incubated with the primary antibody for 30 min at RT. Sections for detection of collagen type II were digested with 1% hyaluronidase (Sigma; H3506-100 MG; in PBS) and 0.2% pronase (Calbiochem, in PBS), each for 15 min at 37°C. Primary antibody was added for 1 h. For detection of aggrecan, sections were pretreated with 0.5 U mL^{-1} chondroitinase ABC (Sigma) in PBS for 30 min at RT and were then incubated with primary antibody for 30 min at RT.

Histopathological evaluation of the biocompatibility index. For the determination of the *in vivo* biocompatibility index (*bi*), septal tissue and surrounding tissue were harvested en bloc. H&E stainings were evaluated according to DIN EN ISO 10993-6, appendix E. Histological characteristics, such as inflammatory reactions, necrosis, fibrosis, fibroplasia, fatty infiltration, and the presence of polymorphous nuclear (PMN) cells, monocytes/macrophages, lymphocytes, plasma, and giant cells were determined in the half-quantitative evaluation system. Based on the histological results, a classification score was estimated for each slide and explant. The integral (whole-number) classification score incorporates the presence and frequency of the different cell types within the implanted scaffold matrix, and in the surrounding tissue. Numbers from 0 to 5 were used for description (0 = absent, 1 = slight, 2 = moderate, 3 = marked, and 4 = severe). The total median and its respective median deviation were calculated for each group and cell type or for the evaluated tissue reaction (fibrosis, fibroplasia, and fatty infiltration). bi_{norm} was defined as the difference between the total median of each time point and the total median of the sham group. To exclude any examination bias, the microscopic analysis and the calculation of *bi* were conducted by using CellMed AG in a double-blind study.

Statistical analysis

The Wilcoxon–Mann–Whitney test was used to evaluate the significance of the *in vitro* cytotoxicity and GAG deposition prior to *in vivo* application ($\alpha = 0.05$). Because the normality test failed, the Kruskal–Wallis one-way analysis of variance on ranks was used for the evaluation of significance (level of significance $\alpha = 0.05$) for cell number, gene expression analysis, GAG deposition, and *bi* ($\alpha = 0.05$). The relative percentage of cell vitality (cytotoxicity testing), the cell number, the relative percentage of GAG content, evaluation of *bi*, and the gene expression are reported as median ± median deviation (MD).

Macroscopic results were statistically analyzed with a multiple logistic regression. Group and time were determining factors, whereas the occurrence of a macroscopically visible septal perforation (yes/no) was the dependent variable. The results were adjusted for the effects of other determining factors in the model to provide "odds ratios" (OR), including *p*-values.

Results

Pore size and E-modulus of marine collagen

SEM analysis of unseeded scaffolds revealed a high porosity and a homogenous pore distribution, with distinct pore interconnectivity visible in the horizontal (Fig. 2a) and vertical cross sections (Fig. 2b). All empty pores in the marine collagen scaffolds had a diameter in the range of 40–200 μm. In horizontal sections of the scaffold center, the pore diameter was 74 ± 18.1 μm. In superficial zones, the pore diameter was 50 ± 20 μm. The E-modulus was between 15 and 25 kPa.

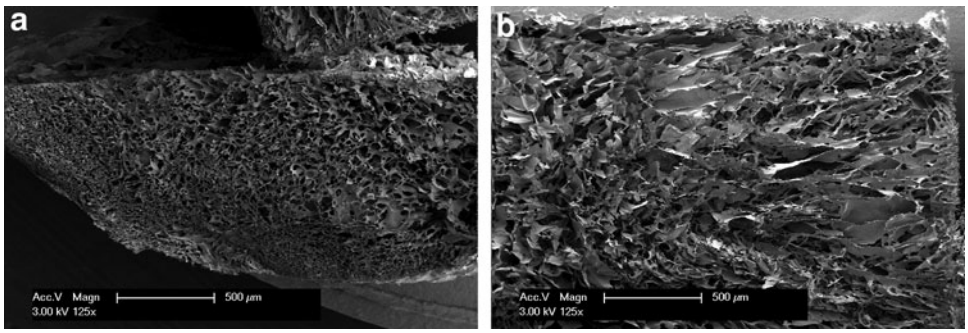

FIG. 2. SEM analysis of marine collagen scaffolds reveals high porosity and homogenous pore distribution on the scaffold surface **(a)** and within the complete scaffold matrix **(b)**. Both views, the superficial top view **(a)** and the vertical cross section, demonstrate the distinct interconnectivity of the scaffold matrix.

Marine collagen is not cytotoxic

The cultivation of L929, rCh and hCh in marine collagen extracts revealed no cytotoxic effects (Fig. 3). Viability for these cell types was 99.65% ± 1.18%, 103.75% ± 1.82%, and 98.24% ± 1.49%, respectively. Cell viabilities between 70% and 100% showed that there were no cytotoxic components in the matrix extracts. The viability of L929 (31.70% ± 5.62%), rCh (26.81% ± 4.88%), and hCh significantly decreased when incubated in DMSO (18.21% ± 2.98%). Cell viabilities between 0% and 40% reflect strong cytotoxic effects. The number of initially seeded cells per each well slightly varied due to technical reasons. Therefore, slightly higher cell numbers cause, as a byproduct, values higher than 100%.

Quantification of human chondrocyte number and GAG production in marine collagen scaffolds

After seeding, the number of adherent hCh was $1.21 \times 10^5 \pm 2.56 \times 10^4$. After 7 ($4.64 \times 10^5 \pm 9.07 \times 10^4$), 14 ($5.22 \times 10^5 \pm 3.77 \times 10^4$), and 21 days ($7.23 \times 10^5 \pm 2.09 \times 10^5$), the cell counts had increased significantly, as determined by the Hoechst assay (Fig. 4a).

Figure 4b shows the significant increase in GAG content (DMMB-assay) during the first week of 3D culture. A GAG content of 3.3 ± 2.35 µg mg^{-1} (per mg dry weight) was measured in native marine collagen scaffolds. After 7 days in culture, the GAG content significantly increased to 19.7 ± 1.9 µg mg^{-1}. After 14 (20.6 ± 2.03 µg mg^{-1}) and 21 days (18.97 ± 2.63 µg mg^{-1}), a slight but not significant increase in GAG content was observed.

Human chondrocytes redifferentiate on marine collagen scaffolds and produce cartilage-specific ECM

Following amplification in monolayer culture, gene expression of all examined ECM markers (*ACAN, COL1A1, COL2A1,* and *VCAN*) was downregulated and detectable only at very low levels. The values of *ACAN, COL1A1, COL2A1,* and *VCAN* expression (0 day) were set to 1 (Fig. 5a, b, dashed threshold line).

After 14 days, *ACAN* expression increased further (*ACAN* 38.25 ± 12.99-fold; each $p < 0.05$) while *COL2A1* expression slightly decreased in comparison to day 7, although still being higher than after monolayer culture (*COL2A1* 14.88 ± 10.60-fold). Between 14 and 21 days, no significant change in gene expression occurred for *COL2A1* and *ACAN*, and a stable expression pattern was detected (*Col2A1* 13.17 ± 18.77-fold; *ACAN* 35.17 ± 17.01-fold).

During the first 7 days of 3D culture, gene expression of *COL1A1* (418.30 ± 180.70-fold) and *VCAN* (86.53 ± 13.93-fold), generally accepted as markers of chondrocyte dedifferentiation,[47] significantly increased compared to day 0 (Fig. 5b). After 14 days, *COL1A1* and *VCAN* expression increased further

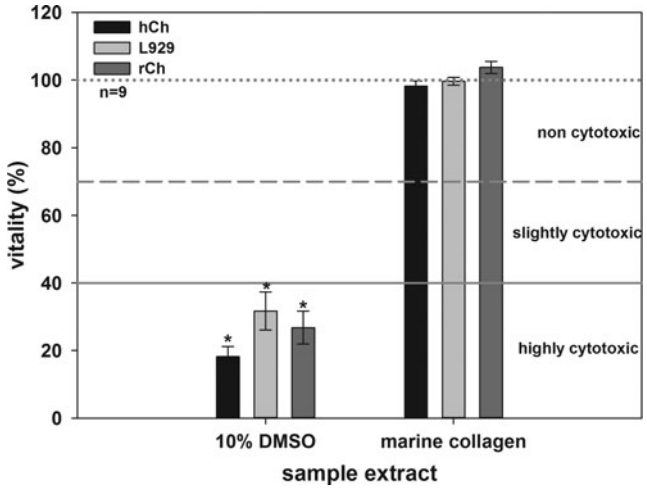

FIG. 3. *In vitro* cytotoxicity test of marine collagen. L929, rCh, and hCh were used as indicator cells. All cells cultured in negative control (dotted line, 100%), or in undiluted sample extracts demonstrate a high viability and reflect the noncytotoxic effect of the extracted marine collagen. No significant differences between negative controls and extracts were detectable. Compared to these results, the cytotoxic effect of 10% DMSO, used as positive control, is significant (each $*p < 0.05$).

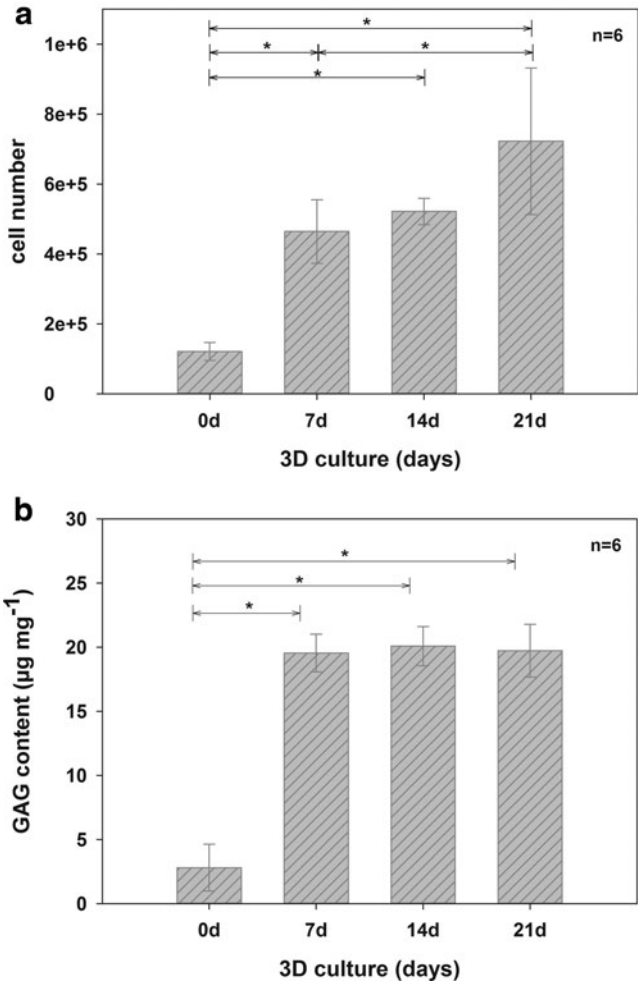

FIG. 4. Changes in cell number **(a)** and content of sGAG **(b)** on marine collagen scaffolds after 0, 7, 14, and 21 days of three dimensional (3D) culture with hCh. Marine collagen scaffolds were initially seeded with 1×10^6 hCh. During 3D culture, the cell number increased significantly. GAG neo synthesis per mg dry weight of unseeded compared to seeded and cultivated scaffolds. GAG synthesis significantly increased during the cultivation period of 21 days, due to enhanced GAG accumulation by human chondrocytes ($*p < 0.05$). sGAG, sulfated glycosaminoglycan

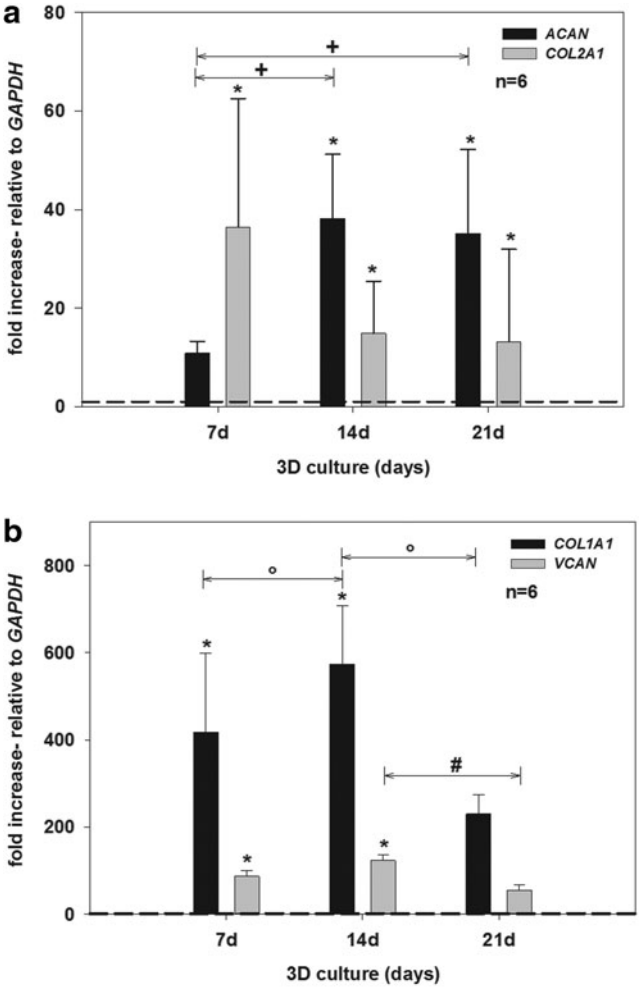

FIG. 5. Relative gene expression of chondrogenic, cartilage-specific marker genes (*ACAN* and *COL2A1*) **(a)**, and marker for dedifferentiation (*COL1A1* and *VCAN*) **(b)**, in 3D culture for 0, 7, 14, and 21 days using hCh. Relative gene expression was calculated by means of the $2^{-\Delta\Delta CT}$ formula. *GAPDH* was used as reference gene and values for *COL2A1, ACAN, COL1A1,* and *VCAN* expression on day 0 (monolayer culture) were set to 1 (dashed threshold line). *COL2A1* and *ACAN* **(a)** were expressed at significantly higher levels compared with day 0 (each $^{*}p<0.05$). With proceeding culture time a significant increase in gene expression of *ACAN* was detected ($^{+}p<0.05$) while expression of *COL2A1* remained on a stable level. Compared to the bench mark of day 0, *VCAN* and *COL1A1* **(b)** expression increased significantly (each $^{*}p<0.05$) during the first 14 days of cultivation. Subsequently, gene expression of both dedifferentiation markers significantly decreased during 3D culture ($^{\circ}$*COL1A1* $p<0.05$; $^{\#}$*VCAN* $p<0.05$).

(*COL1A1* 574.13 ± 134.14-fold; *VCAN* 122.34 ± 14.59-fold; each $p<0.05$). However, after 21 days, gene expression of both of these dedifferentiation markers significantly decreased (*COL1A1* 229.96 ± 43.37-fold; *VCAN* 53.71 ± 12.93-fold; each $p<0.05$).

These results were confirmed by histological and immunohistochemical staining (Fig. 6), and by GAG quantification (Fig. 4b). AB staining (Fig. 6a–c) and specific immunohistochemical staining for aggrecan (Fig. 6d–f) in marine collagen scaffolds seeded with hCh and rCh (data not shown) cultured for up to 21 days allowed the visualization of the enhanced GAG deposition in 3D culture. GAG and aggrecan accumulation was detected by increased staining, starting within the scaffold's periphery where chondrocytes had adhered after seeding. With progressing chondrocyte migration and proliferation, GAG and aggrecan accumulation spread within the scaffold matrix (Fig. 6a–c, d–f).

The capacity of hCh (Fig. 6) and rCh (data not shown) to synthesize ECM products was additionally examined by immunohistochemical staining for collagen type I (Fig. 6j–l) and collagen type II (Fig. 6g–i). Production of collagen type I by hCh was detectable on days 7 (Fig. 6j), 14 (Fig. 6k) and 21 (Fig. 6l). No collagen type II synthesis was detected after 7 days. After 14 and 21 days, collagen type II synthesis increased and progressed to the center of the scaffold as cell migration occurred (Fig. 6g–i). rCh displayed a similar pattern of attachment and ECM neo synthesis (data not shown). The distribution of cell nuclei showed that hCh and rCh initially adhered to the scaffold surface and outer pores of marine collagen. Subsequently, within the first week, both types of chondrocytes migrated to form homogenous cell distributions after 14 and 21 days.

Three dimensional culture of rCh on marine collagen scaffolds prior to in vivo *application enables synthesis of cartilage-specific matrix proteins*

RCh became attached to the scaffold surface. Within 7 days, they migrated throughout the entire scaffold. Aggrecan synthesis increased with culture time from day 1 (Fig. 7a) to day 7 (Fig. 7d). Synthesis of collagen type I (Fig. 7b, e) and type II (Fig. 7c, f) both increased over the culture period. GAG content significantly increased after 7 days (Fig. 8) ($23.54 \pm 2.14\,\mu g\ mg^{-1}$) compared with unseeded scaffolds ($2.81 \pm 1.82\,\mu g\ mg^{-1}$).

Orthotopic animal model for nasal septum replacement, and the frequency of septal perforations

The number of septal perforations was significantly different between the experimental groups. Fewer perforations were detectable within the replacement groups (seeded and unseeded scaffolds) than in the animals of the control group. Specifically, when seeded scaffolds were implanted, none of eight animals had a septal perforation after 1 week. After 4 weeks, three out of seven animals had a perforation, and after 12 weeks, one in eight of the animals had a detectable perforation (Table 2). In animals transplanted with unseeded marine collagen matrices, we found perforations in all 8 individuals after 1 week, in four of six animals after 4 weeks and in three of eight animals after 12 weeks. In the control group, removal of the septal cartilage without replacement resulted in eight of eight animals having a septal perforation after 1 week, six of eight animals having a perforation after 4 weeks and five of seven animals having a perforation after 12 weeks. To prove that the surgical procedure itself does not affect the results, a sham group was established. Following all three explantation time points, no septal perforations were detectable. Furthermore, at all time points, the number of septal perforations was significantly ($p<0.05$) higher in the control group compared to seeded scaffolds. Residual scaffold material was detected in only a few animals. After 1 week, marine collagen remnants were detected by HE staining in the unseeded (5/8) and seeded group (5/10). AB

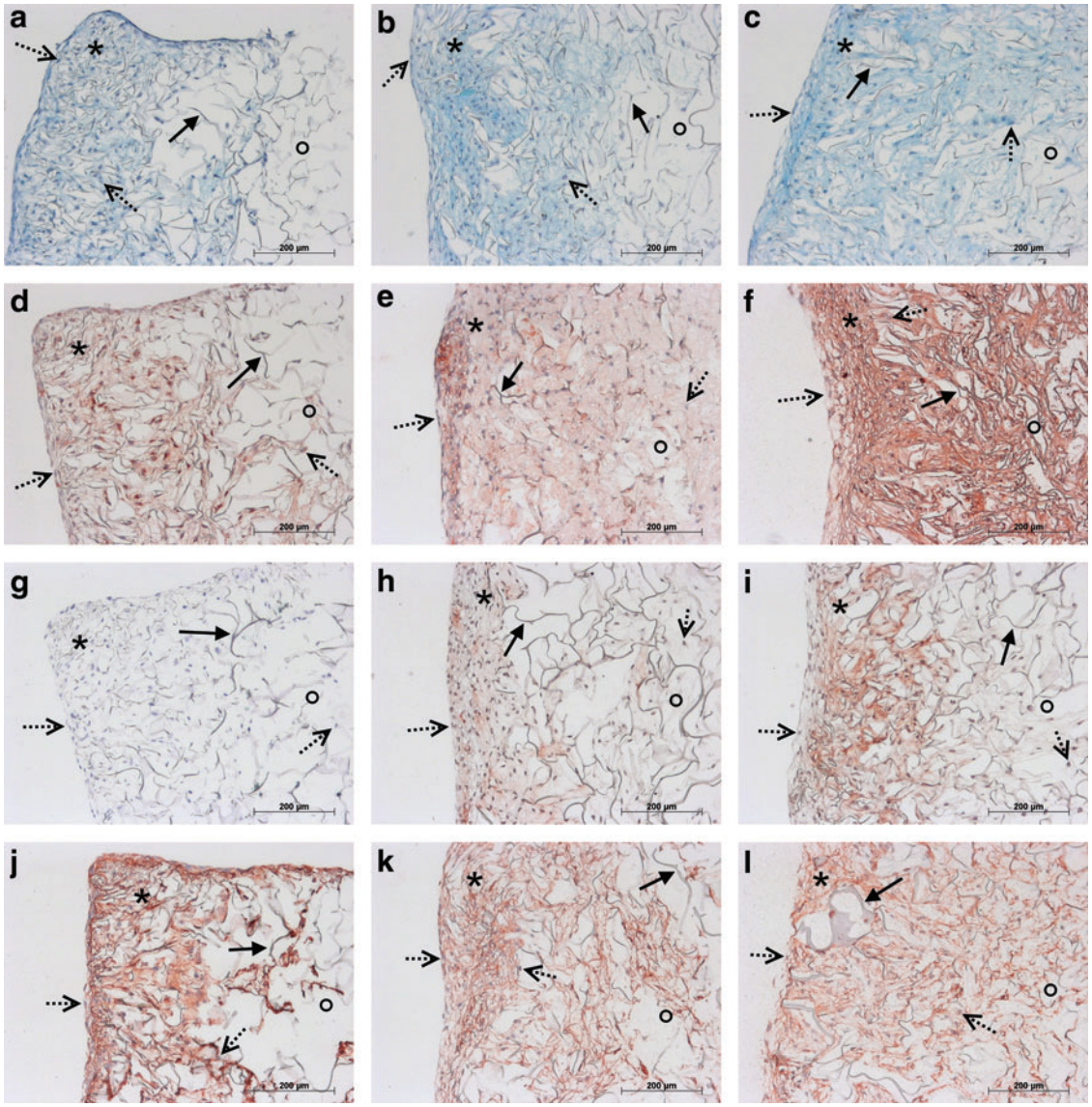

FIG. 6. Histological AB **(a–c)** and immunohistochemical staining for detection of ECM neo synthesis (Agg, collagen type I, and II; **d–l**) in marine collagen scaffolds seeded with hCh starting from day 7 **(a, d, g, j)** until day 14 **(b, e, h, k)** and 21 **(c, f, i, l)**. The AB **(a–c)** staining reflects enhanced GAG deposition during 3D culture. 7 days after seeding **(a)** GAG accumulation was detectable and increased until day 14 **(b)** and 21 **(c)**. A visible increase of GAG and aggrecan accumulation from day 7 **(d)** to day 14 **(e)** and 21 **(f)** was demonstrated. Neo synthesis of collagen type II **(g–i)** started after the first week and visibly increased during further culture after 14 **(h)** and 21 days **(i)**. Collagen type I was present within the whole scaffold starting within one week after initial seeding **(j)** and increasing to day 14 **(k)**. Distribution of collagen type I proceeded into the center of the scaffolds after 21 days. However, the intensity of the staining remained at a comparable level **(l)**. *periphery of scaffold; °center of scaffold; → scaffold fibers; ⇢ cell nuclei. Color images available online at www.liebertpub.com/tea

staining revealed a low level of sGAG synthesis in some of the unseeded scaffolds (Fig. 9). Collagen type I and II were detected in small amounts (data not shown). Furthermore, remnants of marine collagen were detected in two animals of the unseeded group after 4 weeks and in one animal after 12 weeks. Due to the death of 10% of the operated animals, the number of evaluated animals was sometimes lower than eight animals.

Evaluation of the biocompatibility of marine collagen

Changes in total and differential leukocyte frequency with progressing implantation time indicate the presence of acute and chronic inflammatory reactions. PMNs show the acute inflammatory response at shorter times (1 week), whereas increased occurrence of macrophages and lymphocytes indicate persisting chronic inflammatory reactions within the vicinity of implants. PMNs were rarely detected (nearly absent) in all groups and time points. The highest level of PMN infiltration occurred after 1 week in unseeded and seeded scaffolds, and this level decreased until week 12. No significant differences in the median scores of PMNs were found between any of the experimental groups (Table 3).

In all groups, even in the sham group, slight infiltration of lymphocytes and macrophages was detected. Macrophages

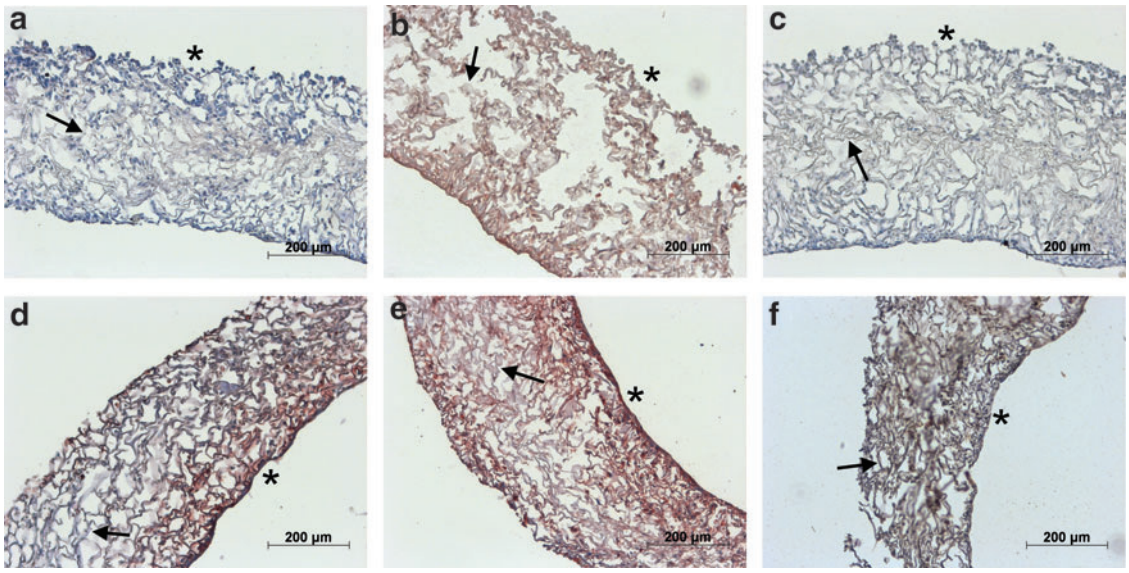

FIG. 7. Marine collagen scaffolds seeded with rCh. While after one day **(a)** aggrecan was not detected, aggrecan deposition (red) became visible after 7 days **(d)**. Collagen type I synthesis visibly increased (red) from day 1 **(b)** to day 7 **(e)**. Within the tightly seeded marine collagen scaffold slight accumulation of collagen type II (brown) **(c,f)** was detectable after 7 days **(f)**. →scaffold fibers; *seeded surface. Color images available online at www.liebertpub.com/tea

and lymphocytes were the dominant cell types in seeded and unseeded scaffolds (Table 3). However, macrophages and lymphocytes were rarely detectable in the sham group. After 1, 4, and 12 weeks, the slight accumulation of macrophages and lymphocytes was significantly higher in unseeded and seeded scaffolds compared to the native cartilage of the sham group ($p < 0.5$) (Table 3). We were not able to detect plasma cells. Giant cells were also very rarely detected. Slight necrosis was observed in seeded and unseeded scaffolds. In unseeded scaffolds, the median necrosis score was (1.50 ± 0.75) after 1 week, and this score significantly decreased after 4 (0.5 ± 0.5) and 12 (0.5 ± 0.5) weeks (each $p < 0.5$). Further, the median necrosis score in 1 (1.0 ± 0.79) and 12 (1.0 ± 0.22) week seeded scaffolds was significantly higher ($p < 0.05$) compared with the 1 (0.0 ± 0.00) and 12 week sham group (0.0 ± 0.24, each $p < 0.5$).

In all experimental animals, low levels of fibroplasia and fibrosis were detectable. One and 4 weeks after implantation, fibrosis in seeded scaffolds (1 week: 2.0 ± 0.35; 4 weeks: 2.00 ± 0.44) was significantly higher than in the sham group (1 week: 1.00 ± 0; 4 weeks: 1.00 ± 0.00; each $p < 0.5$). After 4 (1.00 ± 0.44) and 12 (1.00 ± 0.00) weeks, fibrosis in unseeded scaffolds was significantly higher than in the sham groups (4 weeks: 0.00 ± 0.41; 12 weeks: 0.00 ± 0.41; each $p > 0.5$). Fatty infiltrations were not found in any of the specimens. On the basis of tissue and cellular responses, we determined the *bi* values (Fig. 10a) of the unseeded and seeded scaffolds, and we determined the impact of the surgery itself (sham group). One week after implantation, the *bi* of the unseeded scaffolds (12 ± 1.72) was significantly higher than the *bi* of the sham group (3 ± 1.75, $p < 0.5$), indicating a moderately irritating effect. Until week 12, the *bi* of the unseeded scaffolds significantly decreased to a slightly irritating effect (7.5 ± 0.83, $p < 0.5$). Seeded scaffolds (9 ± 3.16) had a lower (n.s.) *bi* and only slightly irritating effects after 1 week when compared to unseeded scaffolds (12 ± 1.72). The effects of the surgical procedure itself (*bi* of sham group) significantly decreased during the first 4 weeks (1 week: 3 ± 1.75; 4 weeks: 1 ± 0.98, $p < 0.5$). After 4 and 12 weeks, the *bi* of unseeded (4 weeks: 8.5 ± 1.17; 12 weeks: 7.5 ± 0.83, $p < 0.5$) and seeded (4 weeks: 7 ± 1.56; 12 weeks: 8.5 ± 1.00) scaffolds was significantly higher than the *bi* of the sham group (4 weeks: 1 ± 0.98; 12 weeks: 1 ± 1.04, $p < 0.5$).

To separately assess the influence of the seeded and unseeded matrices, the *bi* values were normalized through subtraction of the *bi* evoked by the surgical procedure (sham group). Within 12 weeks, the bi_{norm} (Fig. 10b) decreased to 6.5 (unseeded) and 7.5 (seeded), reflecting the slightly irritating effect of the implants. There were no differences between the groups and time points.

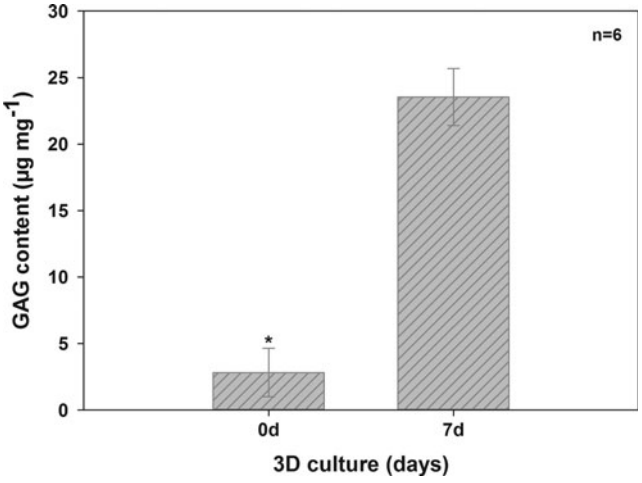

FIG. 8. Presence of GAG in unseeded marine collagen and in scaffolds seeded with rCh. GAG content significantly increased during the cultivation period of 7 days (*$p < 0.05$).

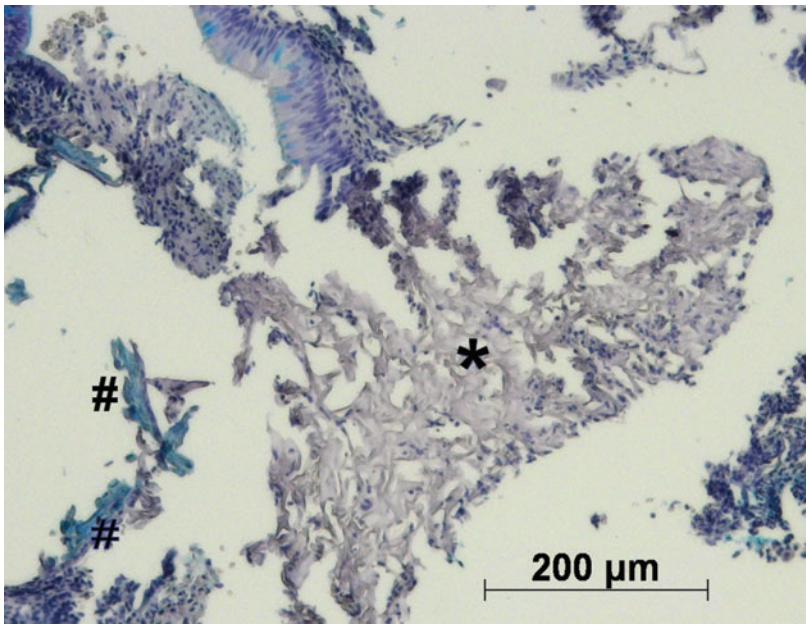

FIG. 9. AB staining of remaining scaffold material (*) of unseeded marine collagen scaffolds after one week *in vivo*. Unseeded collagen scaffolds, demonstrate a slight accumulation of GAGs (#). Color images available online at www.liebertpub.com/tea

Discussion

Cartilage lacks an intrinsic regeneration capacity,[48] which makes cartilage reconstruction challenging. Cartilage reconstruction has become a major focus of tissue engineering research.[19,49] For the first time, this study evaluated the utility of marine collagen as a scaffold for cartilage replacement. We demonstrated that in general, marine collagen scaffolds seem to be suitable cell carriers for clinical cartilage tissue engineering. Further, we established a new immunocompetent rat model for the analysis of tissue-engineered nasal cartilage.

We used triple helical, homotrimer collagen extracted by lyophilization of the jellyfish species *Rhopilema esculentum*.[30] To enhance the mechanical strength, epoxy carbodiimide cross-linking was applied. Various cross-linking reagents, such as formaldehyde, glutaraldehyde, epoxy compounds, carbodiimide (EDC), proanthocyanidin and dimethylsuberimidate, have been used for the fixation and cross-linking of collagen to increase its strength and resistance to enzymatic digestion.[22,50,51] However, all cross-linking agents exhibit certain disadvantages, such as toxicity, instability, and poor control over the rate of cross-linking.[50] Cytotoxicity testing results correlate with short-term implantation studies as

Table 3. Summarized Classification Scores of Seeded and Unseeded Scaffolds 1, 4, and 12 Weeks After Implantation Compared to Sham Group

Group	*Weeks*		*Polymorphnuclear cells*	*Lymphocytes*	*Plasma cells*	*Macrophages*	*Giant cells*	*Necrosis*	*Fibroplasia*	*Fibrosis*	*Fatty infiltrate*
Unseeded	1	Median	0.00	1.00[a]	0.00	1.00[a]	0.00	1.50[a,b]	1.00	1.50[a]	0.00
		±MD	0.22	0.47	0.00	0.22	0.22	0.75	0.00	0.50	0.00
	4	Median	0.00	1.00[a]	0.00	1.00[a]	0.00	0.50	1.00[a]	1.50[a]	0.00
		±MD	0.28	0.28	0.00	0.28	0.00	0.50	0.44	0.50	0.00
	12	Median	0.00	1.00[a]	0.00	1.00[a]	0.00	0.50	1.00[a]	1.50[a]	0.00
		±MD	0.00	0.00	0.00	0.00	0.00	0.50	0.00	0.50	0.00
Seeded	1	Median	0.00	1.00[a]	0.00	1.00[a]	0.00	1.00[a,c]	1.00	2.00[a]	0.00
		±MD	0.59	0.44	0.00	0.20	0.20	0.79	0.20	0.35	0.00
	4	Median	0.00	1.00[a]	0.00	1.00[a]	0.00	0.00	1.00	2.00[a]	0.00
		±MD	0.28	0.00	0.00	0.28	0.28	0.44	0.00	0.44	0.00
	12	Median	0.00	1.00[a]	0.00	1.00[a]	0.00	1.00[a,c]	1.00	1.00	0.00
		±MD	0.22	0.38	0.00	0.22	0.00	0.22	0.22	0.47	0.00
Sham	1	Median	0.00	0.00	0.00	0.00	0.00	0.00	1.00	1.00	0.00
		±MD	0.38	0.38	0.00	0.38	0.38	0.00	0.38	0.00	0.00
	4	Median	0.00	0.00	0.00	0.00	0.00	0.00	0.00	1.00	0.00
		±MD	0.00	0.00	0.00	0.24	0.00	0.41	0.41	0.00	0.00
	12	Median	0.00	0.00	0.00	0.00	0.00	0.00	0.00	1.00	0.00
		±MD	0.00	0.41	0.00	0.00	0.00	0.00	0.41	0.00	0.00

(Classification scores: 0 = absent, 1 = slight, 2 = moderate, 3 = marked, 4 = severe; [a,b,c]$p < 0.05$; [a]compared to respective sham group; [b,c]compared to nonmarked time points of the same group).

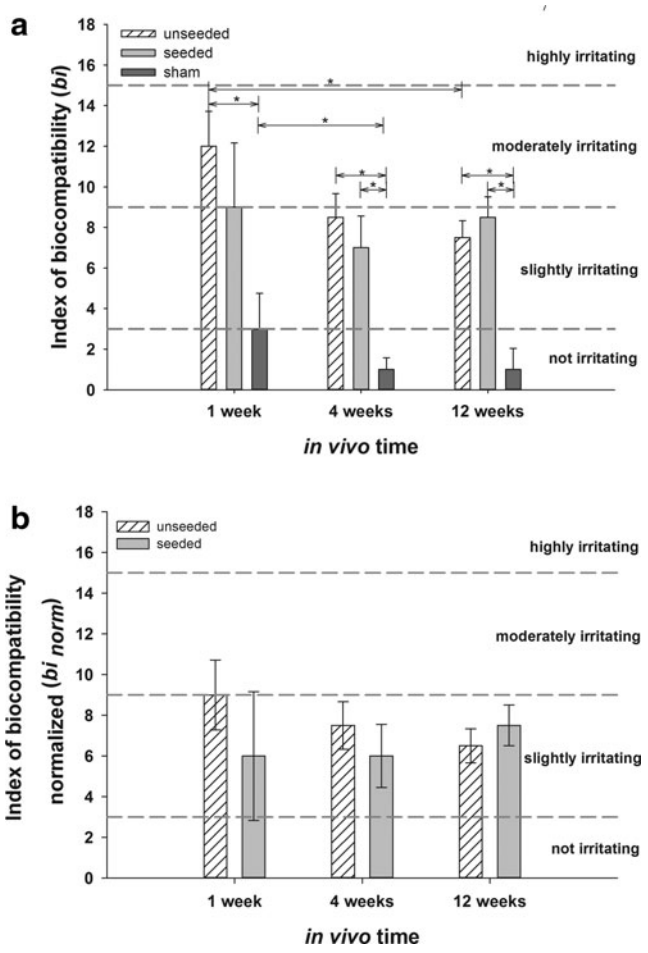

FIG. 10. *bi* and bi_{norm} of seeded and unseeded scaffolds after 1, 4, and 12 weeks as median value ± median deviation compared to sham group **(***bi*, **a)** and after subtraction of the bi of the sham group **(**bi_{norm}, **b)** (*$p < 0.05$). All detected *bi* values are within the slightly irritating range (Classification of *bi*: not irritating 0.0–2.9, slightly irritating 3.0–8.9, moderately irritating 9.0–15.0, and highly irritating >15.1).

Kotzar and coworkers have stated,[52] and the toxicological effects of the marine matrices were first examined *in vitro*. No cytotoxic effects due to material components, EDC cross-linking agents or the production process were detectable, confirming the results presented previously by Song *et al*.[22]

Cross-sections of marine collagen scaffolds revealed high porosity of the scaffold matrices, with distinct interconnectivity, as has been demonstrated previously for other matrices based on jellyfish collagen.[22] The pore size and architecture of biomedical materials are known to influence the diffusivity of nutrients, oxygen and serum in the matrix, and consequently, to control the nutrition of cells.[22,44,53] Furthermore tissue formation[54] and the rate and depth of cellular in growth *in vivo* are also influenced.[55] The pore size of the examined marine collagen scaffolds cannot be rigorously controlled during the freezing process, and thus, varied quite significantly. As estimated by light microscopy, pore size was between 40 and 200 μm, with a main range of 74 ± 18.1 μm in the scaffold center, and 50 ± 20 μm in superficial zones. The literature on optimal pore size for chondrogenesis is quite heterogenous. Some authors favor small pore sizes between 15–50 μm[56] and state that in smaller pore sizes, chondrocytes are packed more closely, and the resulting cell–cell interactions play a key role in phenotype expression.[57] It has been suggested that smaller pore sizes enhance the formation of the ECM and neo cartilage.[58] In contrast, Oh and co-workers[59] state that larger pore sizes (between 380 and 405 μm) are optimal for chondrocytes. These differences are most likely caused by different study designs with respect to cell number and the material used. Other parameters of scaffold architecture design, such as pore shape, porosity, and pore interconnectivity, additionally influence cellular differentiation.[60] In this study, rat and human chondrocytes were detectable on the scaffold surfaces and in the centers of the scaffolds after 7 days. This indicates that despite considerable variability, pore size and pore interconnectivity allowed rapid migration through the scaffold. Therefore, marine collagen scaffolds provide suitable microenvironmental conditions for the homogeneous production of cartilaginous ECM. Rapid GAG synthesis and increased mRNA expression of the cartilage-specific markers collagen type II (gene Col2A1) and aggrecan (Agg) additionally underline this finding.

In addition to pore size, the type of collagen chosen as the implant matrix influences the morphology and phenotype of the chondrocytes. In collagen type I matrices, the expression of phenotype and biosynthetic activity has been shown to be dependent on pore diameter. Most chondrocytes cultured on such matrices retain a fibroblast-like morphology and display an increased proliferation rate with a concomitantly low GAG biosynthetic activity.[57,61] It has been suggested that type II collagen scaffolds provide a better environment for hyaline chondrocytes than collagen type I scaffolds.[61,62] Type II collagen scaffolds facilitate the maintenance of a differentiated chondrocytic phenotype. In collagen type II sponges, bovine and canine chondrocytes have been demonstrated to re-express their typical spherical shape accompanied by the production of cartilage-specific GAG and collagen type II.[61,62] Comparable effects have been demonstrated for rat and human nasal septal chondrocytes in marine collagen matrices within the present study. Both chondrocyte types synthesized GAG and collagen type II in the scaffold, which consists of a homotrimer collagen type similar to collagen type II. Marine collagen possesses only one type of alpha chain and a similar degree of glycosylation compared to vertebrate collagen type II (unpublished results). Although significant production of collagen type I was visualized until day 21 *in vitro*, gene expression analysis demonstrated a shift from collagen type I to collagen type II expression after 21 days. This indicates that chondrogenic redifferentiation with respect to collagen synthesis takes at least 21 days on marine collagen scaffolds. In contrast, aggrecan expression and synthesis is induced already after 7 days in 3D culture.

The *in vitro* results led us to the hypothesis that marine collagen is a suitable material for cartilage tissue engineering. We developed a new model of nasal cartilage repair to evaluate the material for this specific application. To the best of our knowledge, no rat model for nasal cartilage replacement has previously been described. Additionally, no studies are available that use tissue-engineered cartilage in the nasal septum. Tissue replacement in the nose is complicated by the specific immunological environment, which is potentially able to modify material properties[63] and degradation

characteristics. Therefore, a subcutaneous animal model would not meet the requirements of nasal cartilage reconstruction.[63–65] In our study, removal of nasal septal cartilage and reconstruction of that cartilage were carried out in the same procedure. No incisions or flaps of the mucosa were necessary. Thus, the model is comparable to the clinical situation of septum reconstruction, in which septal correction and reconstruction is performed in one step.

Tissue and cellular host responses to local injuries include inflammation, wound healing, and foreign body responses. The host response is initially elicited by the surgical procedure itself.[66,67] For biomedical applications, it is essential to precisely quantify the morphological alterations of cells migrating into the implant matrix[68] and to evaluate the local tissue responses, such as fibrosis or fibroplasia.[52,69] Chronological sequences and pathophysiological tissue responses are used to measure host reactions to implant materials.[67]

During the initial implantation phase, PMNs, leucocytes, and macrophages were detectable in all engineered constructs at low levels. During the chronic inflammatory response, a decreasing level of PMNs was detected. A slight infiltration of macrophages and lymphocytes was detectable throughout the entire experiment, indicating a slightly irritating effect on the marine collagen scaffold. As with many other biocompatible materials,[66] the inflammatory response to our implants revealed low levels of macrophages, which fused to form foreign body giant cells, after 1 (unseeded and seeded) and 4 weeks (seeded). Granulation tissue development, foreign body reaction, and fibrosis (fibrous capsule) vary in duration, depending on degradation rate.[66] Due to the high *in vivo* biodegradability of marine collagen,[22] rapid phagocytosis of marine collagen by macrophages and foreign body giant cells took place within the first 4 weeks after implantation. The cellular infiltration scores and *bi* classification of marine collagen were low, indicating an overall minor irritating effect and slight tissue and cellular inflammation responses.

The prevention of septal perforations is an important issue in clinical septal reconstruction. After 1 week, septal perforation occurred in 100% of the animals when the nasal septum was not replaced (control group), and it occurred in more than 70% of the animals of the control group after 12 weeks. These data are comparable to the clinical situation, in which perforations occur frequently when septal cartilage is not replaced.

In contrast to the results of Kaiser *et al.*,[70] no regenerative areas were found in our model in samples of the control group. In their study, the authors used a rabbit model and studied cartilaginous regeneration after 7 months. Thus, the different study design can explain the differences in results. To exclude septal perforations that occurred due to surgical technique, the sham group was established, and no perforations were detectable.

Although, there was no significant difference between the groups implanted with seeded and unseeded scaffolds after 4 and 12 weeks, we detected significantly fewer perforations when the nasal septum was replaced by seeded scaffolds in comparison to the control group. This indicates the positive effect of seeded scaffolds for the effective prevention of septal perforations. This is emphasized by the significant difference between seeded and unseeded scaffolds after 1 week. Our results suggest that septal replacement by seeded marine collagen matrices is more effective because less perforations were detectable with seeded matrices. Therefore, seeding with chondrocytes is an important factor in nasal cartilage engineering, at least under the experimental conditions used in this model. Overall, the *in vivo* results indicate that marine collagen is a promising new scaffold for nasal cartilage tissue engineering.

Time seems to be an additional factor influencing septal perforations, as confirmed by the observation that after 12 weeks, fewer perforations were detectable than after 1 week in the unseeded scaffold group. Spontaneous regeneration, as demonstrated by Kaiser *et al.*[70] in their rabbit model after 7 months, was not detected histologically but might have reduced the number of septal perforations. This is supported by the tests of unseeded marine collagen scaffolds.

The rapid biodegradability of marine collagen has been demonstrated earlier[22] and was confirmed by our data. The relatively low biomechanical stiffness of the material[22] necessitated careful handling during surgery but did not disturb the biological function of the implants. More complete cross-linking of the marine collagen could be helpful from a surgical point of view.

In summary, our findings indicate that marine collagen is a safe, natural collagen matrix without cytotoxic effects. At the same time, marine collagen offers excellent biocompatibility, with only slight evidence of local inflammatory reactions. Scaffolds are suitable for effectively preventing nasal septal perforations, especially when seeded with autologous chondrocytes. Thus, marine collagen is a promising candidate for cartilage tissue engineering. The newly established rat model can be used to compare the properties of various biomaterials for orthotopic nasal cartilage repair.

Acknowledgments

The collagen type II antibody (II-II6B3; isotype mouse IgG1) was obtained from the Developmental Studies Hybridoma Bank, developed under the auspices of the NICHD and maintained by the University of Iowa, Department of Biological Sciences, Iowa City, IA 52242.

The authors acknowledge the excellent technical assistance of M. Jerg, K. Urlbauer, G. Cudek, and V. Fuss (CellMed AG, Alzenau, Germany). Special thanks to Birgit Hoyer (Carl Gustav Carus University Medical Center and Medical Department of the Technical University Dresden, Germany) for providing the SEM images.

The work was supported by a grant from the European Commission (EXPERTISSUES, Contract No. 500283) and by CRM (Coastal Research & Management, Kiel, Germany).

Disclosure Statement

No competing financial interests exist.

References

1. Rotter, N., Haisch, A., and Bucheler, M. Cartilage and bone tissue engineering for reconstructive head and neck surgery. Eur Arch Otorhinolaryngol **262,** 539, 2005.
2. Mandl, E.W., Jahr, H., Koevoet, J.L., van Leeuwen, J.P., Weinans, H., Verhaar, J.A., and Van Osch, G.J. Fibroblast growth factor-2 in serum-free medium is a potent mitogen and reduces dedifferentiation of human ear chondrocytes in monolayer culture. Matrix Biol **23,** 231, 2004.
3. Rotter, N., Bucheler, M., Haisch, A., Wollenberg, B., and Lang, S. Cartilage tissue engineering using resorbable scaffolds. J Tissue Eng Regen Med **1,** 411, 2007.

4. Nagata, S. Modification of the stages in total reconstruction of the auricle: Part I. Grafting the three-dimensional costal cartilage framework for lobule-type microtia. Plast Reconstr Surg **93,** 221, 1994.
5. Ohara, K., Nakamura, K., and Ohta, E. Chest wall deformities and thoracic scoliosis after costal cartilage graft harvesting. Plast Reconstr Surg **99,** 1030, 1997.
6. Ryan, M.W., and Quinn, F.B., Jr. Advancing otolaryngology education in the new millennium. Otolaryngol Clin North Am **40,** 1191, 2007.
7. Wang, J.H., Lee, B.J., and Jang, Y.J. Use of silicone sheets for dorsal augmentation in rhinoplasty for Asian noses. Acta Otolaryngol Suppl **558,** 115, 2007.
8. Sevin, K., Askar, I., Saray, A., and Yormuk, E. Exposure of high-density porous polyethylene (Medpor) used for contour restoration and treatment. Br J Oral Maxillofac Surg **38,** 44, 2000.
9. Stone, K.R., Rodkey, W.G., Webber, R.J., McKinney, L., and Steadman, J.R. Future directions. Collagen-based prostheses for meniscal regeneration. Clin Orthop Relat Res **252,** 129, 1990.
10. Glowacki, J., and Mizuno, S. Collagen scaffolds for tissue engineering. Biopolymers **89,** 338, 2008.
11. O'Brien, F.J., Harley, B., Yannas, I.V., and Gibson, L.J. The effect of pore size on cell adhesion in collagen-GAG scaffolds. Biomaterials **26,** 433, 2005.
12. Wakitani, S., Kimura, T., Hirooka, A., Ochi, T., Yoneda, M., Yasui, N., Owaki, H., and Ono, K. Repair of rabbit articular surfaces with allograft chondrocytes embedded in collagen gel. J Bone Joint Surg Br **71,** 74, 1989.
13. Langer, R., and Vacanti, J.P. Tissue engineering. Science **260,** 920, 1993.
14. Vacanti, C.A., Langer, R., Schloo, B., and Vacanti, J.P. Synthetic polymers seeded with chondrocytes provide a template for new cartilage formation. Plast Reconstr Surg **88,** 753, 1991.
15. Freed, L., Marquis, J., Nohria, A., Emmanual, J., Mikos, A., and Langer, R. Neocartilage formation *in vitro* and *in vivo* using cells cultured on synthetic biodegradable polymers. J Biomed Mater Res A **27,** 11, 1993.
16. Chia, S.H., Schumacher, B.L., Klein, T.J., Thonar, E.J., Masuda, K., Sah, R.L., and Watson, D. Tissue-engineered human nasal septal cartilage using the alginate-recovered-chondrocyte method. Laryngoscope **114,** 38, 2004.
17. Liese, J., Marzahn, U., El Sayed, K., Pruss, A., Haisch, A., and Stoelzel, K. Cartilage tissue engineering of nasal septal chondrocyte-macroaggregates in human demineralized bone matrix. Cell Tissue Bank 1, 2012.
18. Kusuhara, H., Isogai, N., Enjo, M., Otani, H., Ikada, Y., Jacquet, R., Lowder, E., and Landis, W.J. Tissue engineering a model for the human ear: assessment of size, shape, morphology, and gene expression following seeding of different chondrocytes. Wound Repair Regen **17,** 136, 2009.
19. Cao, Y., Vacanti, J.P., Paige, K.T., Upton, J., and Vacanti, C.A. Transplantation of chondrocytes utilizing a polymer-cell construct to produce tissue-engineered cartilage in the shape of a human ear. Plast Reconstr Surg **100,** 297, 1997.
20. Mafi, P., Hindocha, S., Mafi, R., and S Khan, W. Evaluation of biological protein-based collagen scaffolds in cartilage and musculoskeletal tissue engineering- a systematic review of the literature. Curr Stem Cell Res Ther **7,** 302, 2012.
21. Tuli, R., Li, W.J., and Tuan, R.S. Current state of cartilage tissue engineering. Arthritis Res Ther **5,** 235, 2003.
22. Song, E., Yeon Kim, S., Chun, T., Byun, H.J., and Lee, Y.M. Collagen scaffolds derived from a marine source and their biocompatibility. Biomaterials **27,** 2951, 2006.
23. Lee, C.H., Singla, A., and Lee, Y. Biomedical applications of collagen. Int J Pharm **221,** 1, 2001.
24. Friess, W. Collagen—biomaterial for drug delivery. Eur J Pharm Biopharm **45,** 113, 1998.
25. Riesle, J., Hollander, A., Langer, R., Freed, L., and Vunjak-Novakovic, G. Collagen in tissue-engineered cartilage: Types, structure, and crosslinks. J Cell Biochem **71,** 313, 1998.
26. Sano, A., Maeda, M., Nagahara, S., Ochiya, T., Honma, K., Itoh, H., Miyata, T., and Fujioka, K. Atelocollagen for protein and gene delivery. Adv Drug Deliv Rev **55,** 1651, 2003.
27. Ma, L., Gao, C., Mao, Z., Zhou, J., and Shen, J. Enhanced biological stability of collagen porous scaffolds by using amino acids as novel cross-linking bridges. Biomaterials **25,** 2997, 2004.
28. Murray, M.M., Rice, K., Wright, R., and Spector, M. The effect of selected growth factors on human anterior cruciate ligament cell interactions with a three-dimensional collagen-GAG scaffold. J Orthop Res **21,** 238, 2003.
29. Angele, P., Abke, J., Kujat, R., Faltermeier, H., Schumann, D., Nerlich, M., Kinner, B., Englert, C., Ruszczak, Z., and Mehrl, R. Influence of different collagen species on physico-chemical properties of crosslinked collagen matrices. Biomaterials **25,** 2831, 2004.
30. Addad, S., Exposito, J.Y., Faye, C., Ricard-Blum, S., and Lethias, C. Isolation, characterization and biological evaluation of jellyfish collagen for use in biomedical applications. Mar Drugs **9,** 967, 2011.
31. Exposito, J.Y., Valcourt, U., Cluzel, C., and Lethias, C. The fibrillar collagen family. Int J Mol Sci **11,** 407, 2010.
32. In Jeong, S., Kim, S.Y., Cho, S.K., Chong, M.S., Kim, K.S., Kim, H., Lee, S.B., and Lee, Y.M. Tissue-engineered vascular grafts composed of marine collagen and PLGA fibers using pulsatile perfusion bioreactors. Biomaterials **28,** 1115, 2007.
33. Hayashi, Y., Yamada, S., Yanagi Guchi, K., Koyama, Z., and Ikeda, T. Chitosan and fish collagen as biomaterials for regenerative medicine. Adv Food Nutr Res **65,** 107, 2012.
34. Lin, Z., Solomon, K.L., Zhang, X., Pavlos, N.J., Abel, T., Willers, C., Dai, K., Xu, J., Zheng, Q., and Zheng, M. *In vitro* evaluation of natural marine sponge collagen as a scaffold for bone tissue engineering. Int J Biol Sci **7,** 968, 2011.
35. Duda, G.N., Haisch, A., Endres, M., Gebert, C., Schroeder, D., Hoffmann, J.E., and Sittinger, M. Mechanical quality of tissue engineered cartilage: results after 6 and 12 weeks *in vivo*. J Biomed Mater Res **53,** 673, 2000.
36. Homicz, M.R., Schumacher, B.L., Sah, R.L., and Watson, D. Effects of serial expansion of septal chondrocytes on tissue-engineered neocartilage composition. Otolaryngol Head Neck Surg **127,** 398, 2002.
37. Brittberg, M., Lindahl, A., Nilsson, A., Ohlsson, C., Isaksson, O., and Peterson, L. Treatment of deep cartilage defects in the knee with autologous chondrocyte transplantation. N Engl J Med **331,** 889, 1994.
38. Kafienah, W., Jakob, M., Demarteau, O., Frazer, A., Barker, M.D., Martin, I., and Hollander, A.P. Three-dimensional tissue engineering of hyaline cartilage: comparison of adult nasal and articular chondrocytes. Tissue Eng **8,** 817, 2002.
39. Malda, J., Kreijveld, E., Temenoff, J.S., Blitterswijk, C.A., and Riesle, J. Expansion of human nasal chondrocytes on macroporous microcarriers enhances redifferentiation. Biomaterials **24,** 5153, 2003.
40. Naumann, A., Rotter, N., Bujia, J., and Aigner, J. Tissue engineering of autologous cartilage transplants for rhinology. Am J Rhinol **12,** 59, 1998.
41. Stok, K.S., Lisignoli, G., Cristino, S., Facchini, A., and Müller, R. Mechano-functional assessment of human mesenchymal stem

cells grown in three-dimensional hyaluronan-based scaffolds for cartilage tissue engineering. J Biomed Mater Res A **93,** 37, 2010.
42. Schwarz, S., Koerber, L., Elsaesser, A.F., Goldberg-Bockhorn, E., Seitz, A.M., Durselen, L., Ignatius, A., Walther, P., Breiter, R., and Rotter, N. Decellularized cartilage matrix as a novel biomatrix for cartilage tissue-engineering applications. Tissue Eng Part A **18,** 2195, 2012.
43. Kim, Y.J., Sah, R.L., Doong, J.Y., and Grodzinsky, A.J. Fluorometric assay of DNA in cartilage explants using Hoechst 33258. Anal Biochem **174,** 168, 1988.
44. Schwarz, S., Elsaesser, A.F., Koerber, L., Goldberg-Bockhorn, E., Seitz, A.M., Bermueller, C., Durselen, L., Ignatius, A., Breiter, R., and Rotter, N. Processed xenogenic cartilage as innovative biomatrix for cartilage tissue engineering: effects on chondrocyte differentiation and function. J Tissue Eng Regen Med, 2012.
45. Barbosa, I., Garcia, S., Barbier-Chassefiere, V., Caruelle, J.P., Martelly, I., and Papy-Garcia, D. Improved and simple micro assay for sulfated glycosaminoglycans quantification in biological extracts and its use in skin and muscle tissue studies. Glycobiology **13,** 647, 2003.
46. Livak, K.J., and Schmittgen, T.D. Analysis of Relative Gene Expression Data Using Real-Time Quantitative PCR and the $2^{-\Delta\Delta CT}$ Method. Methods **25,** 402, 2001.
47. Lin, Z., Fitzgerald, J.B., Xu, J., Willers, C., Wood, D., Grodzinsky, A.J., and Zheng, M.H. Gene expression profiles of human chondrocytes during passaged monolayer cultivation. J Orthop Res **26,** 1230, 2008.
48. Ciorba, A., and Martini, A. Tissue engineering and cartilage regeneration for auricular reconstruction. Int J Pediatr Otorhinolaryngol **70,** 1507, 2006.
49. Vacanti, C.A., Cima, L.G., Ratkowski, D., Upton, J., and Vacanti, J.P. Tissue engineered growth of new cartilage in the shape of a human ear using synthetic polymers seeded with chondrocytes. MRS Proc **252,** 1991.
50. Han, B., Jaurequi, J., Tang, B.W., and Nimni, M.E. Proanthocyanidin: a natural crosslinking reagent for stabilizing collagen matrices. J Biomed Mater Res A **65,** 118, 2003.
51. Hey, K., Lachs, C., Raxworthy, M., and Wood, E. Crosslinked fibrous collagen for use as a dermal implant: control of the cytotoxic effects of glutaraldehyde and dimethylsuberimidate. Biotechnol Appl Biochem **12,** 85, 1990.
52. Kotzar, G., Freas, M., Abel, P., Fleischman, A., Roy, S., Zorman, C., Moran, J.M., and Melzak, J. Evaluation of MEMS materials of construction for implantable medical devices. Biomaterials **23,** 2737, 2002.
53. Nuernberger, S., Cyran, N., Albrecht, C., Redl, H., Vécsei, V., and Marlovits, S. The influence of scaffold architecture on chondrocyte distribution and behavior in matrix-associated chondrocyte transplantation grafts. Biomaterials **32,** 1032, 2011.
54. Roosa, S.M.M., Kemppainen, J.M., Moffitt, E.N., Krebsbach, P.H., and Hollister, S.J. The pore size of polycaprolactone scaffolds has limited influence on bone regeneration in an *in vivo* model. J Biomed Mater Res A **92,** 359, 2009.
55. Zeltinger, J., Sherwood, J.K., Graham, D.A., Müeller, R., and Griffith, L.G. Effect of pore size and void fraction on cellular adhesion, proliferation, and matrix deposition. Tissue Eng **7,** 557, 2001.
56. Aigner, T., and Stove, J. Collagens—major component of the physiological cartilage matrix, major target of cartilage degeneration, major tool in cartilage repair. Adv Drug Deliv Rev **55,** 1569, 2003.
57. Nehrer, S., Breinan, H.A., Ramappa, A., Young, G., Shortkroff, S., Louie, L.K., Sledge, C.B., Yannas, I.V., and Spector, M. Matrix collagen type and pore size influence behaviour of seeded canine chondrocytes. Biomaterials **18,** 769, 1997.
58. Stenhamre, H., Nannmark, U., Lindahl, A., Gatenholm, P., and Brittberg, M. Influence of pore size on the redifferentiation potential of human articular chondrocytes in poly (urethane urea) scaffolds. J Tissue Eng Regen Med **5,** 578, 2011.
59. Oh, S.H., Park, I.K., Kim, J.M., and Lee, J.H. *In vitro* and *in vivo* characteristics of PCL scaffolds with pore size gradient fabricated by a centrifugation method. Biomaterials **28,** 1664, 2007.
60. Jeong, C.G., and Hollister, S.J. Mechanical and biochemical assessments of three-dimensional poly (1, 8-octanediol-co-citrate) scaffold pore shape and permeability effects on *in vitro* chondrogenesis using primary chondrocytes. Tissue Eng Part A **16,** 3759, 2010.
61. Nehrer, S., Breinan, H.A., Ramappa, A., Shortkroff, S., Young, G., Minas, T., Sledge, C.B., Yannas, I.V., and Spector, M. Canine chondrocytes seeded in type I and type II collagen implants investigated *in vitro*. J Biomed Mater Res **38,** 95, 1997.
62. Pieper, J.S., van der Kraan, P.M., Hafmans, T., Kamp, J., Buma, P., van Susante, J.L., van den Berg, W.B., Veerkamp, J.H., and van Kuppevelt, T.H. Crosslinked type II collagen matrices: preparation, characterization, and potential for cartilage engineering. Biomaterials **23,** 3183, 2002.
63. Kunisawa, J., Fukuyama, S., and Kiyono, H. Mucosa-associated lymphoid tissues in the aerodigestive tract: their shared and divergent traits and their importance to the orchestration of the mucosal immune system. Curr Mol Med **5,** 557, 2005.
64. Yun, K., and Moon, H.T. Inducing chondrogenic differentiation in injectable hydrogels embedded with rabbit chondrocytes and growth factor for neocartilage formation. J Biosci Bioeng **105,** 122, 2008.
65. Lattyak, B.V., Maas, C.S., and Sykes, J.M. Dorsal onlay cartilage autografts. Arch Facial Plast Surg **5,** 240, 2003.
66. Anderson, J.M., and Langone, J.J. Issues and perspectives on the biocompatibility and immunotoxicity evaluation of implanted controlled release systems. J Controlled Release **57,** 107, 1999.
67. Anderson, J.M., and Shive, M.S. Biodegradation and biocompatibility of PLA and PLGA microspheres. Adv Drug Deliv Rev **28,** 5, 1997.
68. Garosi, G., and Di Paolo, N. The rabbit model in evaluating the biocompatibility in peritoneal dialysis. Nephrol Dial Transplant **16,** 664, 2001.
69. International Organization of Standardization. Biological Evaluation of Medical Devices - Part 5: Tests for *In Vitro* Cytotoxicity; (ISO 10993-5:2009); German version EN ISO 10993-5:2009, 2009.
70. Kaiser, M.L., Karam, A.M., Sepehr, A., Wong, H., Liaw, L.L., Vokes, D.E., and Wong, B.J. Cartilage regeneration in the rabbit nasal septum. Laryngoscope **116,** 1730, 2006.

Address correspondence to:
Silke Schwarz, MSc
Department of Otorhinolaryngology
Ulm University Medical Center
Frauensteige 12
Ulm 89075
Germany

E-mail: silke.schwarz@uniklinik-ulm.de

Received: November 2, 2012
Accepted: April 16, 2013
Online Publication Date: June 4, 2013